

DESIGNING AND OPTIMIZING A MICROMANIPULATOR-CONTROLLED SURGICAL TOOL FOR REPRODUCIBLE NERVE CRUSH INJURIES IN MICE

Connor Mullen – M2¹, Haney M², Hinkel C¹, Deninger I¹, Welby L¹, Ukatu C¹, and Lever TE¹

¹Department of Otolaryngology – Head and Neck Surgery, ²Veterinary Pathobiology
University of Missouri School of Medicine

INTRODUCTION

Recurrent laryngeal nerve (RLN) injury, even if temporary, is a devastating complication of anterior cervical surgical procedures, resulting in debilitating dysphonia and dysphagia. During surgery, injury can be imparted by stretching, crushing, cauterizing, and/or transecting the laryngeal nerves. The injury can be temporary or permanent, depending on the severity and mechanism of insult. Treatment of the injury is generally palliative in nature and includes feeding tubes, voice and swallowing therapy, and diet modifications.

The underlying pathophysiology of RLN is not completely understood. To effectively investigate various treatment strategies in mouse models, we need to improve the current translational animal model by standardizing the widely-used manual nerve crush techniques that apply variable force and may unintentionally add traction injuries. **To control for these potential confounds, we are developing a micromanipulator-controlled surgical tool that (1) reliably applies a calibrated crush force injury, and (2) minimizes secondary injuries, such as traction, induced by manual methods.**

METHODS

Crush Force Analysis: The crush force was analyzed using TekScan's Flexiforce Economical Load and Force (ELF) System. Following calibration (Figure 1), the crushing force of the smooth, curved hemostat (FST, Foster City, CA), aneurysm clip (Sugita Titanium aneurysm clip Mizuho, Tokyo, Japan), and crush tool were quantified.

Crush Tool Metrics: Based on literature and surgical observations, the size and parameters of the device tips were made to accommodate an RLN diameter of ~100 μm.

Crush Tool Fabrication: Ethicon's EBF02 Laparoscopic Bipolar Electrode was identified as the best tool for the following modifications: making the tips the appropriate size, fabricating a lever system to transduce energy produced by a solenoid, and automating the crush duration by developing a custom controller.

Electrical/Power Component Development: The controller consists of three components: a microcontroller, a variable voltage regulator, and a display. The microcontroller is based on an ATmega U34-Arduino Pro Micro that allows for control over the crush duration while being amendable to user input via a rotary encoder. Output voltage is controlled by a variable voltage regulator. The character LCD display offers user feedback when setting the crush duration and throughout the crush.

Surgical Implementation of the Crush Tool: Mice were deeply anesthetized and an incision was made along the anterior aspect of the superior neck. The RLN was visualized alongside the trachea, and isolated. After isolation, the crush tool was maneuvered to the ideal location – between the 5-6th tracheal rings, the nerve was draped over the tips, and a crush was performed.

METHODS



Figure 1 Calibration. Calibrating the force sensor, TekScan's Flexiforce ELF System, involved multiple steps. **A: Preparing the sensor.** After inserting the sensor (black arrow) into its adaptor (white asterisk), it first needed to be "broken in," which involved applying a force with one's finger that maxed out the default force settings 3-4 times. **B: Weight calibration.** First the force reading was zeroed. Next, based on the approximate force being tested, a predetermined maximum weight (ex. 1000 g) was applied to the sensor on top of a small 3D printed disk (blue arrow) that ensured the entire weight was detected by the force sensor, and the sensitivity setting was optimized. Then, each of the three predetermined weights (ex. 1000 g, 500 g, 200 g) were set on the printed disk 5 times. With those 15 data points, the Flexiforce ELF System computed a linear relationship to analyze the unknown crush forces. **C: Crush force analysis set-up.** Left to Right: Smooth, curved hemostat (green arrow), Aneurysm clip (yellow arrow), Crush tool (red arrow). Each method underwent 20 crush trials, and the average, standard deviation (StdDv), and 95% confidence interval (C.I.) were measured. The crush tool's dimensions required a non-centered force reading. To remain consistent, the crush force of the hemostat and aneurysm clip were analyzed over the same area of the sensor as the crush tool.

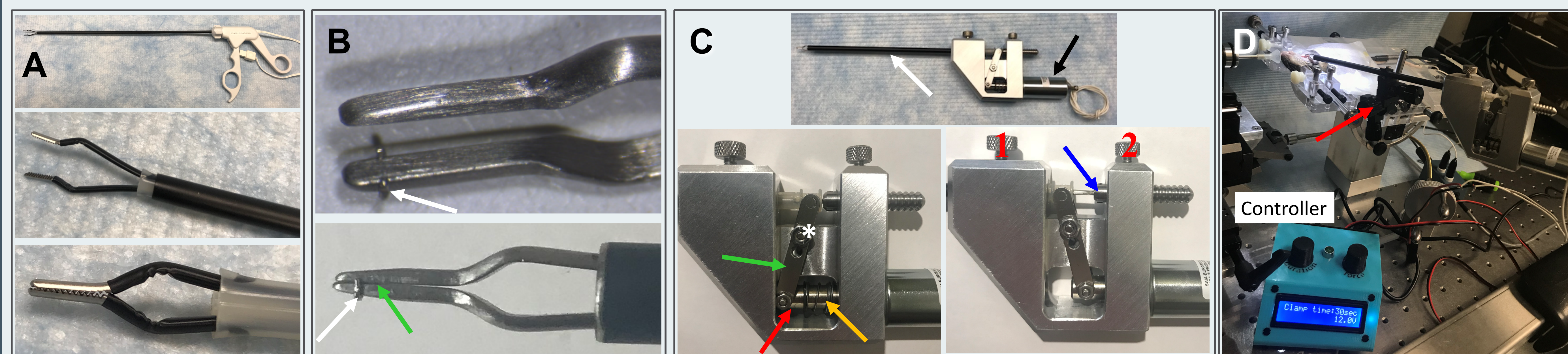


Figure 2 Device Fabrication. **A:** The original Ethicon's EBF02 Laparoscopic Bipolar Electrode. **Top:** Entire tool, unmodified. **Middle:** Tips of the laparoscopic tool in the resting position. **Bottom:** Clamping of the laparoscopic tips. **B: Laparoscopic tip modifications.** The serrated tips were molded into smooth tips to provide a more consistent crushing surface and additional mechanical stability. "Securing hooks" (white arrows) were added to ensure each nerve underwent the same crush injury. The tip length measured 7 mm, the inferior tip thickness was 2 mm, and the tip width was decreased from 1.85 mm to 1.25 mm. **Top:** Tips in resting position. **Bottom:** Tips closed, highlighting the flush tip faces (green arrow). **C: Lever mechanism to transduce solenoid energy to the crush tips.** Close-up of the lever mechanism. The lever mechanism is powered by a linear pull solenoid (black arrow). When powered, the solenoid pulls the plunger (red arrow) proximally. The plunger is connected to the long arm of the lever (green arrow) that pivots around the fulcrum (white asterisk). This pivoting provides the torque necessary to distally extend the plastic sheath encasing the superior and inferior tips causing them to clamp flush together. The two springs (yellow arrow) around the solenoid plunger provide the force required to reset the lever to its original position. The tips are anchored (blue arrow) to provide stability. Two thumb screws (numbered 1 and 2 in red) allow for adjustment of the tip location with respect to how far they extend beyond the aluminum outer-tube (white arrow). **Top:** Prototype crush tool disconnected from power supply. **Bottom Left:** Starting position, solenoid not fired. **Bottom Right:** Crushing position, solenoid fired. **D: In vivo use of the crush tool.** Connected to the crush tool is the controller (blue box, labeled). The controller allows for the delivery of a consistent crush force for a predetermined amount of time (e.g., 30 seconds). The crush tool is mounted on a micromanipulator (red arrow) that provides 3 degrees of freedom along three perpendicular axes (x, y, and z).

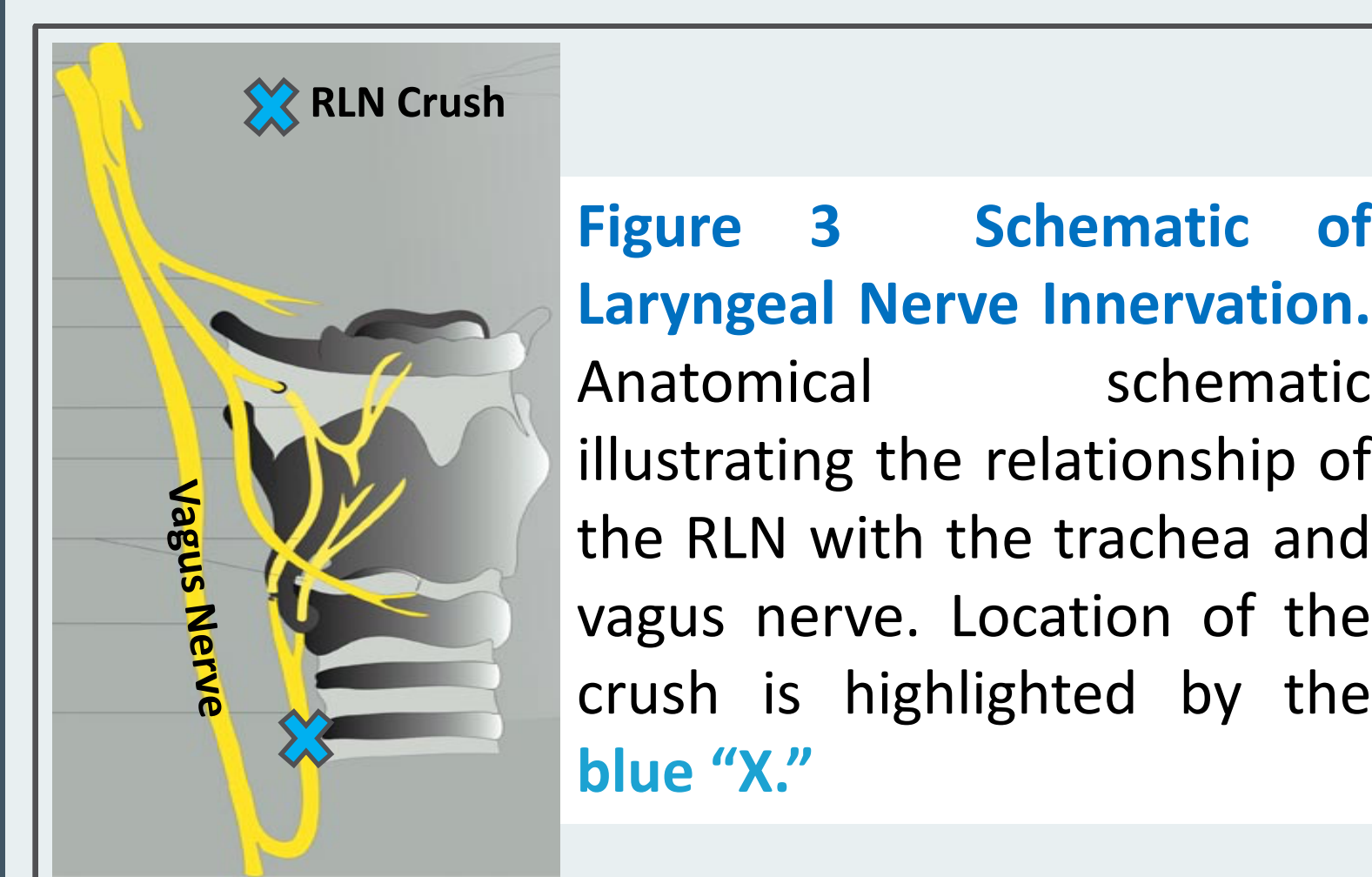


Figure 3 Schematic of Laryngeal Nerve Innervation. Anatomical schematic illustrating the relationship of the RLN with the trachea and vagus nerve. Location of the crush is highlighted by the blue "X."

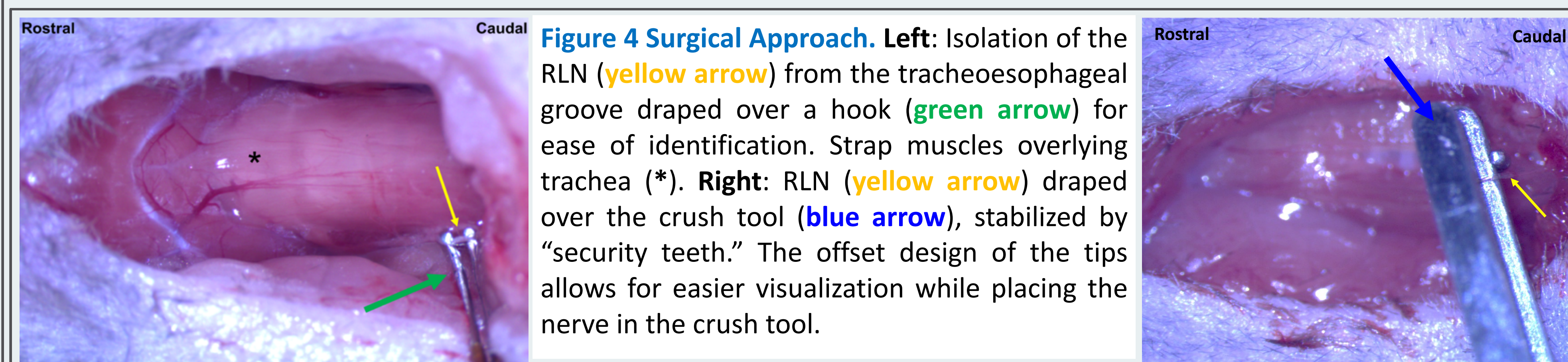
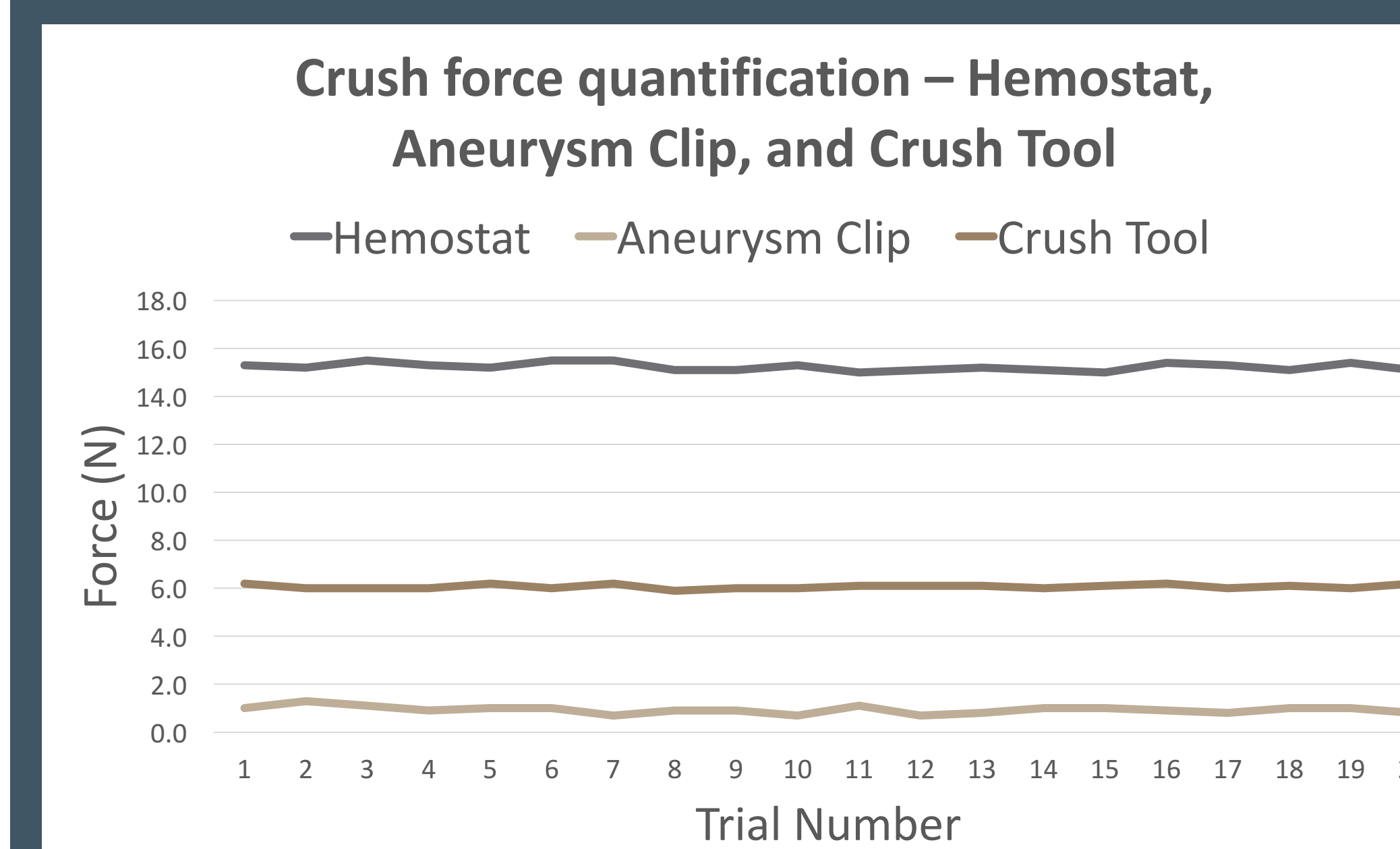


Figure 4 Surgical Approach. **Left:** Isolation of the RLN (yellow arrow) from the tracheoesophageal groove draped over a hook (green arrow) for ease of identification. Strap muscles overlying trachea (*). **Right:** RLN (yellow arrow) draped over the crush tool (blue arrow), stabilized by "security teeth." The offset design of the tips allows for easier visualization while placing the nerve in the crush tool.

CONCLUSIONS

- We successfully designed and prototyped a micromanipulator-controlled surgical tool for reproducible nerve crush injuries in mice.
- Based on preliminary data, our crush tool provides a more consistent crush force compared to the smooth, curved hemostat and the aneurysm clip. The more consistent crush will improve the RLN nerve crush injury mouse model used for our ongoing investigations of various treatment modalities.
- Crush force analysis of the hemostat and aneurysm clip helps explain previous experimental differences in post-nerve crush injury outcomes between the two modalities.

RESULTS



TRIAL ANALYSIS			
	Hemostat	Aneurysm Clip	Crush Tool
Average (Newton)	15.2	0.9	6.1
StdDv	0.16	0.15	0.09
CI	0.079	0.066	0.04

Figure 5 Consistency and Quantification of Crush Force. The hemostat's average crush force when "two-clicks" were used was 15.2 N (n = 20, StdDv = 0.16, CI = 0.070). The average crushing force of our Sugita Titanium aneurysm clip with a manufacturer calibrated 1.3 N crush force (Tessem B, et al., 2009) was 0.9 N (n = 20, StdDv = 0.15, CI = 0.066). Our new crush tool's average crush force was 6.1 N (n = 20, StdDv = 0.09, CI = 0.040).

FUTURE DIRECTIONS

- Our new crush tool will be used to improve the current mouse model for investigating the efficacy of intraoperative nerve stimulation of the vagus and the main trunk of the facial nerve following a unilateral crush injury.
- Current analysis of RLN crush injury includes: pre- and post-surgery laryngoscopy to visualize the vocal folds, analysis of their movement using custom automated tracking software, and post-crush transmission electron microscopy (TEM) to assess the degree of nerve damage.

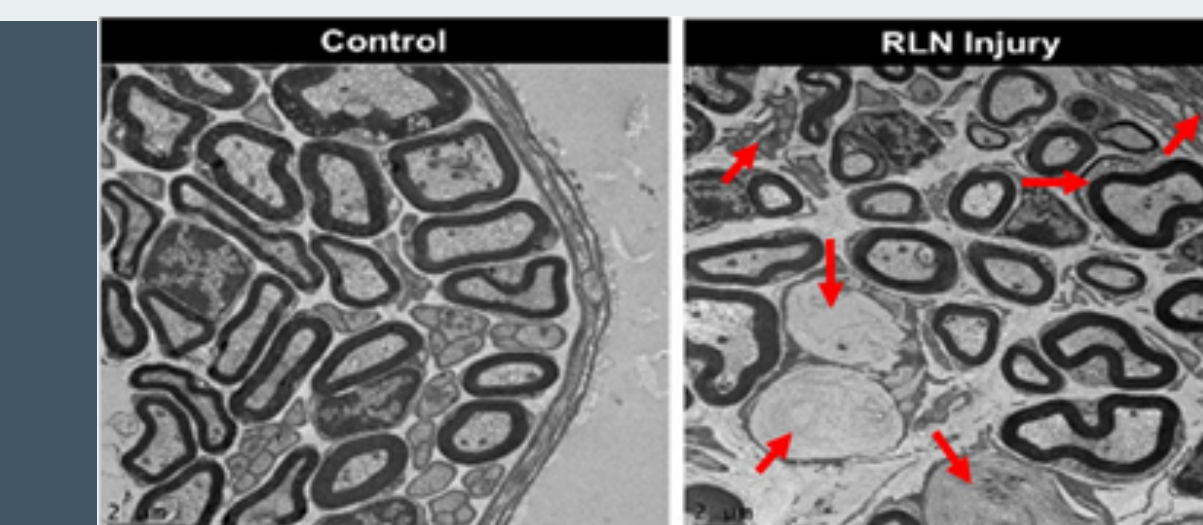


Figure 6 Representative cross-sectional TEM images of the distal RLN post-surgery in mice. Compared to control (uninjured, Left) samples, striking RLN degeneration (red arrows) was readily apparent in RLN crush injury samples (Right). Evidence of degeneration included: excess collagen, cellular debris, mitochondrial degeneration & displacement, redundant myelination, etc.

ACKNOWLEDGMENTS

- Roderic Schlotzhauer (Physics Machine Shop) for fabrication and design assistance
- Kate Osman (Lever Lab) for managing the mouse colony for this project.
- MU School of Medicine Summer Research Fellowship Award (Connor Mullen)
- Project funded in large part by NIH T-32 stipend (Megan Haney)